TÜBİTAK

Turkish Journal of Earth Sciences

http://journals.tubitak.gov.tr/earth/

Research Article

Turkish J Earth Sci
(2017) 26: 421-440

doi:10.3906/yer-1702-11

Feather-like hornblende aggregates in the phyllites from the southern Sanandaj–Sirjan zone, Iran; their origin and mode of formation

Hossein FATEHI[1], Hamid AHMADIPOUR[2,*], Nakashima KUZUO[2], Hesamaddin MOEINZADEH[1]
[1]Department of Geology, Faculty of Sciences, Shahid Bahonar University of Kerman, Kerman, Iran
[2]Department of Earth and Environmental Sciences, Yamagata University, Kojirakawa-Machi, Japan

Received: 16.02.2017 • **Accepted/Published Online:** 25.10.2017 • **Final Version:** 23.11.2017

Abstract: Several outcrops of spectacular feather-like hornblende aggregates occur in the phyllites of the Gol-e-Gohar complex (southeast of Iran) and form special Garbenschiefer rock types. The Gol-e-Gohar complex, as a part of the southern Sanandaj–Sirjan metamorphic zone, contains a succession of metabasites, phyllites, and slates intruded by dioritic intrusions. There are two types of hornblendes in the phyllites; the first one is concentrated around the fractures and the second one is randomly distributed in the rocks and forms radial feather-like hornblende aggregates. Petrographical and chemical characteristics of these two shapes of hornblendes are the same, except the latter is developed parallel to the foliation planes. The hornblendes occur as unstrained needle-shaped porphyroblasts with oriented quartz and feldspar inclusions as well as polygonal grains in the matrix with mosaic texture, which implies the matrix has been recrystallized. On the basis of field observations, petrography, and chemical compositions of the hornblendes, we inferred that the Garbenschiefer phyllites formed during hydrothermal metamorphism in association with penetration of hot fluids. The compositions of hornblende aggregates are similar to those formed in hydrothermal systems and differ from regional and thermal metamorphic amphiboles. All evidence shows that, in the studied area, ascending of dioritic intrusions increases fluid temperature, the hot fluids leach some elements from the metabasites, and finally the enriched fluids flow upward via the fractures. In the upper levels, the fluids penetrate into the phyllites along their foliation planes and, with a decrease in temperature and pressure, they crystallize hornblende aggregates under static hydrothermal conditions.

Key words: Garbenschiefer, Gol-e-Gohar complex, feather-like hornblende, Iran, phyllite, Sanandaj–Sirjan metamorphic zone

1. Introduction

Amphibole as an important constituent of the middle to the lower crust (Kirby and Kronenberg, 1987; Ranalli and Murphy, 1987; Berger and Stunitz, 1996) can be formed by several processes. During regional and thermal metamorphisms, the first appearance of this mineral occurs at the transition from sub-greenschist to greenschist facies (Robinson et al., 1982; Bevins and Robinson, 1994; Schumacher, 2007; Bucher and Grapes, 2011). In addition, it can be crystallized directly by fluid–rock interaction during hydrothermal metamorphism, when the temperatures of fluids correspond to those considered for upper sub-greenschist to greenschist facies (Springer and Day, 2002).

One of the spectacular shapes of amphiboles in metamorphic rocks is Garbenschiefer (feather-like) hornblende aggregates. Development of feather-like hornblendes has been described from a number of occurrences (Bierman, 1977; Rosing et al., 1996; Komiya et al., 1999; Rosing, 1999; Polat et al., 2002; Furnes et al., 2009; Steffen et al. 2014). Their development is explained by two main mechanisms: (1) a succession of weakening and strengthening episodes (Steffen et al. 2014) and (2) deformation and metamorphism, which together exert control on fluid availability, diffusion rate, and reaction kinetics (Furnes et al., 2009). Some evidence in the present study suggests other factors such as the role of fluids and fluid pathways for the formation of these hornblende aggregates. Fluid–rock interaction in the contact aureoles of acidic intrusions can occur at 550–600 °C (Buick and Cartwright, 1994; Buick et al., 1994a) and up-temperature fluid flows have been proposed for several regionally metamorphosed terrains such as the Reynolds Range and Mount Lofty Ranges, Australia (Cartwright et al., 1995), and Vermont, USA (Ferry, 1992; Stern et al., 1992; Leger and Ferry, 1993).

In the southeast of the Sanandaj–Sirjan metamorphic zone (south of Kerman Province, Iran), there are feather-like radial aggregates of hornblende formed in the phyllites of the Gol-e-Gohar metamorphic complex. The nature and

* Correspondence: hahmadi@uk.ac.ir

origin of these aggregates have not been understood yet. The present study was conducted to investigate the field and petrographical characteristics of these phenomena along with the chemical compositions of the hornblendes and their mode of formation. For this purpose, we use field observations, petrographical features, and the mineral chemistry to show the role of channeled infiltration of hot fluids and fluid–rock interaction in the formation of amphibole-bearing Garbenschiefer phyllites in the Gol-e-Gohar complex.

2. Geological setting

The study area is a part of the southeastern Sanandaj–Sirjan metamorphic zone and is located in Kerman Province, southeast Iran (Figure 1a). This zone is characterized by Paleozoic metamorphic and complexly deformed rocks and abundant deformed and undeformed Mesozoic plutons (Mohajjel et al. 2003). In the south of the Sanandaj–Sirjan zone, the Paleozoic units were deformed and metamorphosed in different stages (Berberian and King, 1981; Sabzehei et al., 1997b; Sheikholeslami, 2008; Arfani and Shahriari, 2009). These units consist of the Gol-e-Gohar, Rutchun, and Khabr complexes (Figure 1b). According to stratigraphic relations, the oldest unit (protolith) belongs to the Gol-e-Gohar metamorphic complex, which is lower Paleozoic (Cambrian) in age (Sabzehei et al., 1997a). This complex contains slate, phyllite, micaschist, metabasites, and quartzite and hosts the studied Garbenschiefer rock types. These units are overlain by the Rutchun and Khabr complexes. Unmetamorphosed Mesozoic units containing shale, sandstone, conglomerate, and basaltic and andesitic lava flows crop out mainly in the northern part of this

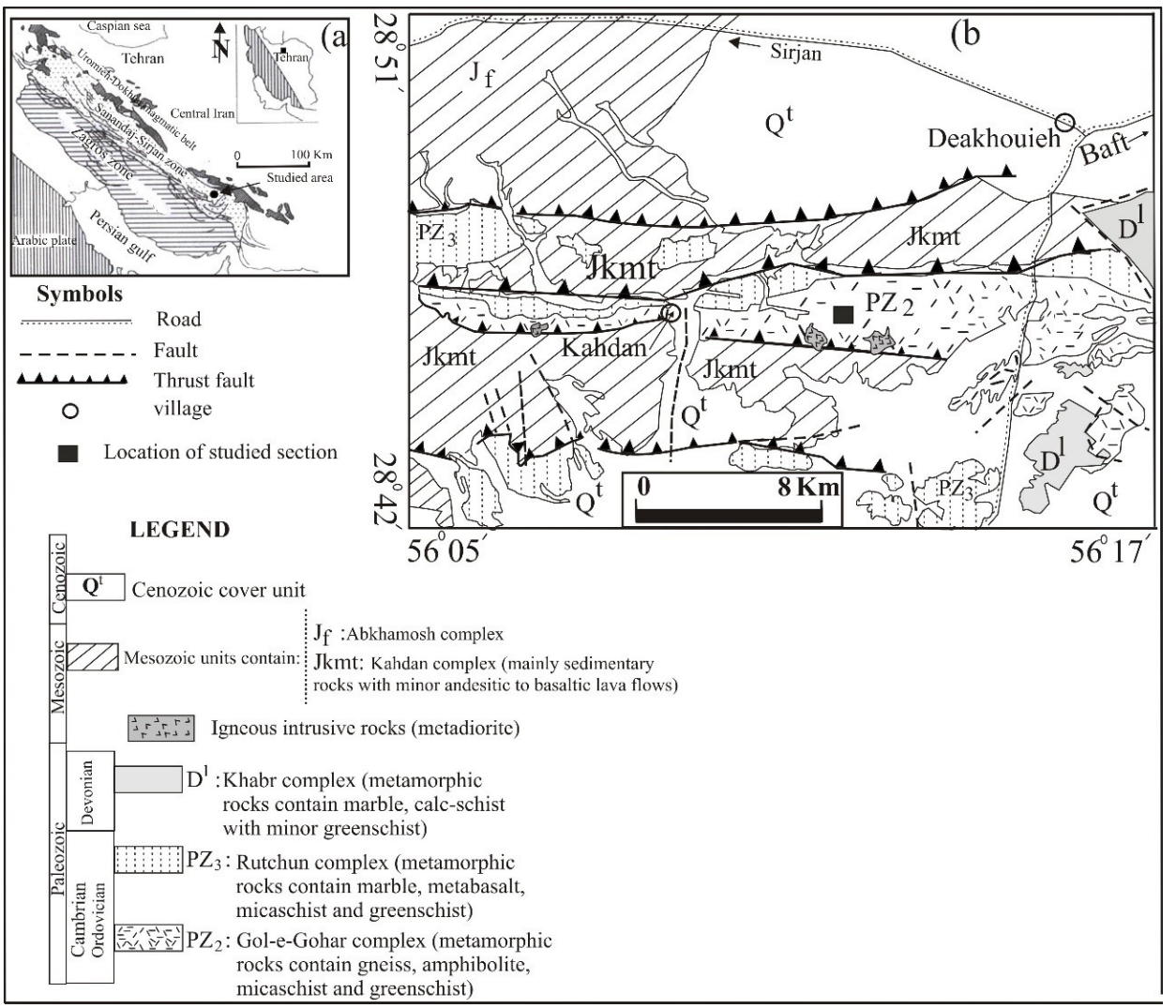

Figure 1. a: Geological situation of the study area in Iran (Mohajjel and Fergusson, 2000). b: Simplified geological map of the study area (Sabzehei et al., 1997b) showing locations of the studied column.

area (Figure 1b). The Gol-e-Gohar metamorphic complex, in which Garbenschiefer phyllites occur, contains metasedimentary rocks (slates, phyllites, and micaschists), metabasites (amphibole-schist), metalimestone, and pegmatitic rocks (muscovite tourmaline pegmatite). Small patches of meta-diorites occur sporadically in these units.

3. Analytical methods

For electron microprobe analyses, several polished-thin sections were prepared from the Gol-e-Gohar Garbenschiefer-shaped phyllites that host hornblende radial aggregates. In these sections, garnet, amphibole, muscovite, epidote, chlorite, ilmenite, plagioclase, and quartz were analyzed. Chemical compositions were obtained using a JEOL JXA-8600 M electron microprobe micro-analyzer (EPMA) at the EMS Laboratory of Yamagata University in Japan with an accelerating voltage of 15 kV, a beam current of 20 nA, and count times of 10 s. In order to investigate the exact chemical variations in amphiboles, several micro-traverses have been done parallel and perpendicular to the long axes of amphibole grains.

4. Results

4.1. Field relationships

Because feather-like amphiboles occur in the phyllites and metabasites of the Gol-e-Gohar complex, field characteristics of these units are interpreted with more detail in a measured stratigraphic column (Figure 2). This column is located in the southwest of Deakhouieh village with a longitude of 56°14′11″ and latitude of 28°45′18″. Layers show a strike of N 80 W and dip of 55 NE. As shown in the column of Figure 2, Garbenschiefer phyllites occur between other porphyroblast-free phyllites alternatively.

In the lowermost part of the column, an amphibole schist (metabasite) unit (Sabzehei et al., 1997b) crops out. This unit is invaded by several Triassic diorite intrusions (Sabzehei et al., 1997b) occurring either as apophyses (up to 40 m in diameter) or dikes (up to 5 m in thickness). These intrusions have metamorphosed in greenschist facies and intruded into the metamorphic units of the Gol-e-Gohar complex and contain small crystals of biotite, feldspar, and amphibole. Upwards, there is an alternation of slate, phyllite, and metabasite units and then, toward the top of the column, a thick outcrop of metabasite layers and crosscutting meta-granites occurs. Veins and veinlets of secretory quartzites are found in all of the units. The metabasite rocks are seen as black to dark-gray and dark to light-green rocks (Figure 3a). In these rocks, preferably oriented plagioclase and amphibole porphyroblasts are seen. Some features such as abundant amphiboles and plagioclases along with the enrichment of iron and magnesium minerals show that they are probably metabasites formed by metamorphism of basic igneous rocks.

In the studied area, there are several outcrops of phyllites and slates of the Gol-e-Gohar Paleozoic complex. Slates occur as layered dark-gray rocks in alternation with the other rock units, up to 80 m in thickness, and contain fine foliation, slaty cleavage, kink banding, and folding. Downward, the phyllites appear as gray rocks with well-developed foliation. These shiny phyllites occur as anastomosing discontinuous layers up to 100 m in thickness and show irregular successions with slates, schists, and meta-limestones. They show a distinctive foliation in which the fine-grained micas have been crystallized parallel to the foliation and, in some parts, scattered garnet porphyroblasts give them an appearance similar to spotted phyllites. These phyllites are characterized by their kink bands, folding, and feather-like hornblende aggregates. In the field, they have very fine-grained garnet, biotite, and muscovite (Figure 3b). Some of these Garbenschiefer phyllites contain (feather-like) hornblende radial porphyroblasts (up to 10 cm in length) with random distributions and orientations. They crystallized parallel to the foliation planes and indicate broomstick and radial shape hornblende grains (Figure 3c). Sporadic garnet porphyroblasts (up to 1.5 cm in diameter) and chlorite (up to 3 mm) crystals are also found in the phyllites (Figure 3d), whereas in the slates, flake-like amphibole porphyroblasts are smaller (up to 3 mm long) than those in phyllites and lack any radial shapes. The study of metamorphic events and deformation phases in the Gol-e-Gohar complex shows that the rock units have experienced three metamorphic events and four deformation phases.

4.2. Petrographical features

Metamorphosed mafic rocks of the Gol-e-Gohar complex contain chlorite, epidote, sphene, amphibole, biotite, and plagioclase (Figure 4a). Slates and phyllites are fine-grained rocks in which primary layering (S_0) appears as an alternation of light quartz-feldspar-rich and dark chlorite-muscovite- and graphite-rich bands. In these rocks, S_1 foliation is defined by primary quartz, feldspar, chlorite, and opaque minerals stretched and orientated as a result of deformation. In addition, new minerals have been formed as small muscovite, biotite, and garnet crystals in these rocks. S_1 foliation is a continuous foliation generated parallel to the primary layering (Figure 4b). In those rocks, S_2 foliation has developed pervasively, while S_1 foliation just occurs as inclusion trails in garnet minerals and/or as fine-grained minerals in the matrix with a different orientation relative to the S_2. In order to understand the relation between crystallization of the hornblende aggregates and regional metamorphism in the area, metamorphic events and deformation phases in the area are described

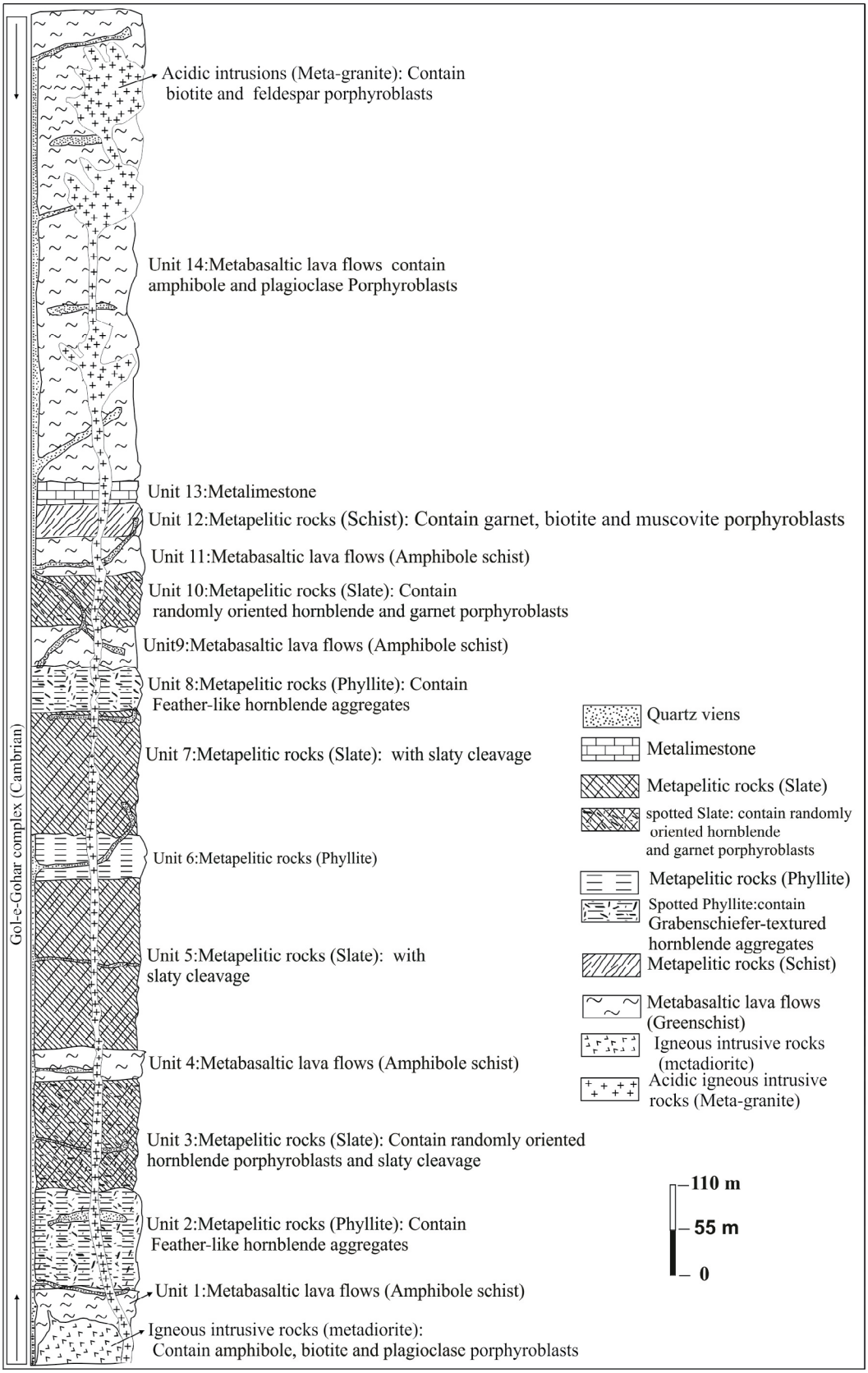

Figure 2. Measured stratigraphic column of the Gol-e-Gohar complex metamorphic units in the study area.

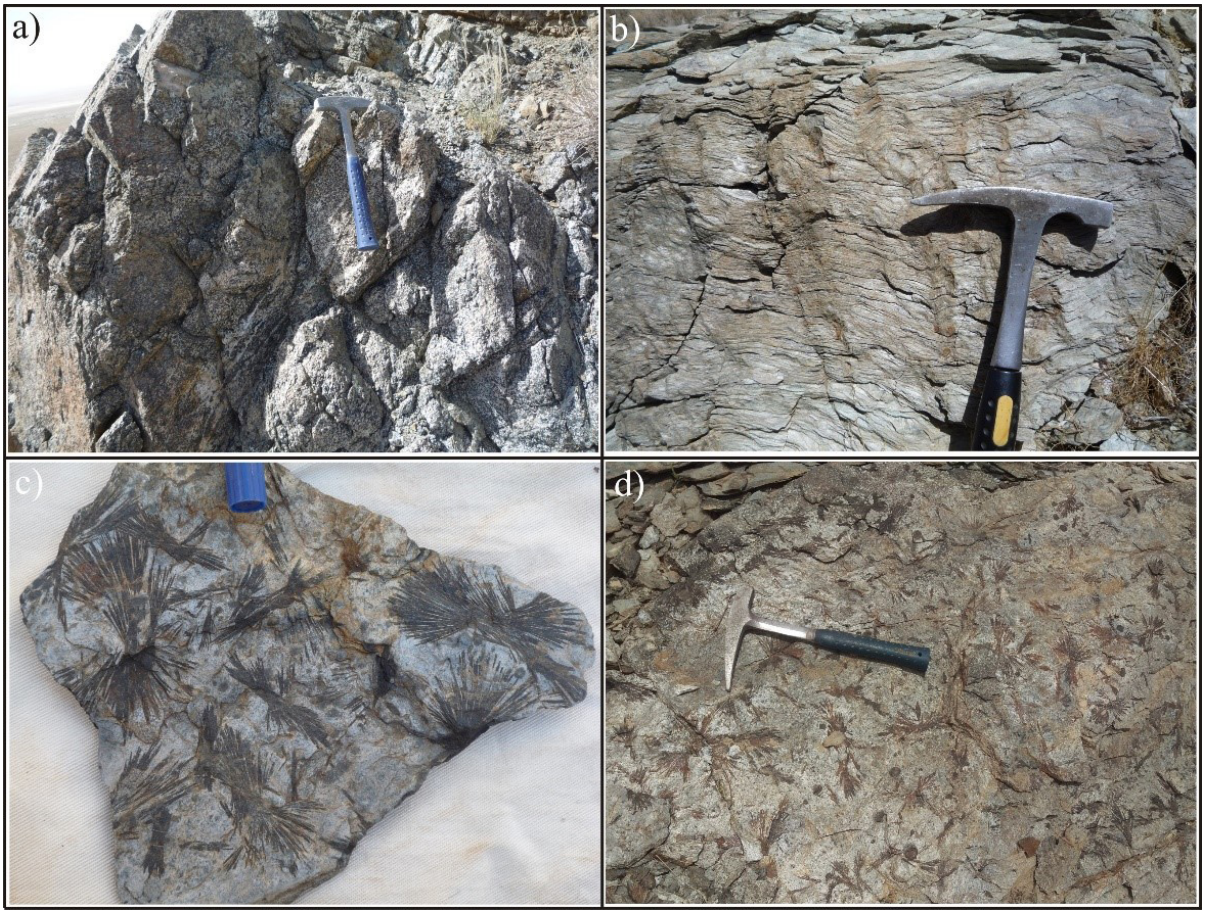

Figure 3. Field characteristics of rock units in the study area, a: Gol-e-Gohar amphibole-schist (metabasite) outcrop contains alternations of light and black bands with ribbon texture. b: Hornblende-free fine-grained phyllites from the Gol-e-Gohar complex. c: Feather-like hornblende porphyroblasts in the Garbenschiefer phyllite. d: An outcrop from the Gol-e-Goharphyllites with garnet porphyroblasts and feather-like hornblende aggregates.

briefly. In the first metamorphic event, which is associated with the first deformation phase, muscovite, biotite, and garnet minerals were formed and oriented along the first schistosity (S1) just parallel to the primary layering (Figure 4b). The second metamorphic event acted simultaneously with the second deformation phase and led to overgrowth of the previous porphyroblasts and re-orientation of them parallel to the second schistosity. The third metamorphic event, which is associated with the third deformation phase, produced fine-grained muscovite along the shear zones and probably dioritic intrusions that acted as heat sources for the formation of hornblende radial aggregates, intruded during this stage at the middle-late Triassic period (228 m.a.) (Fatehi, 2017). Then the feather-like hornblende appears and overprints some of the previous records (Figure 4c). The last deformation phase produced normal, reverse, and thrust faults in a brittle condition.

Petrographically, feather-like hornblende-bearing phyllite hosting hornblende radial aggregates contain hornblende, garnet, quartz, feldspars, epidote, ilmenite, chlorite, and small amounts of calcite. The most outstanding features in these rocks are radial, broomstick-shaped hornblende aggregates crystallized on the foliation plane. These crystals distribute randomly and heterogeneously throughout the rocks. They occur as needle-like crystalline aggregates nucleated from a point and grown in two opposite directions (Figure 4c). The length of these needles reaches even 10 cm, while their widths are only a few millimeters (with aspect ratios of 3:1 to 7:1) and sometimes they show intersecting relationships (Figure 4c). They appear as green to brownish-green porphyroblasts containing a larger number of oriented fined-grained quartz-feldspar inclusions (Figure 4d). There are no deformational features or preferred orientation in the hornblende crystals, and so they can be post-tectonic porphyroblasts formed after a strong schistosity and envelope small oriented crystals as inclusion trails. However, in the matrix and on the outside of these porphyroblasts, coarse-grained quartz-feldspar

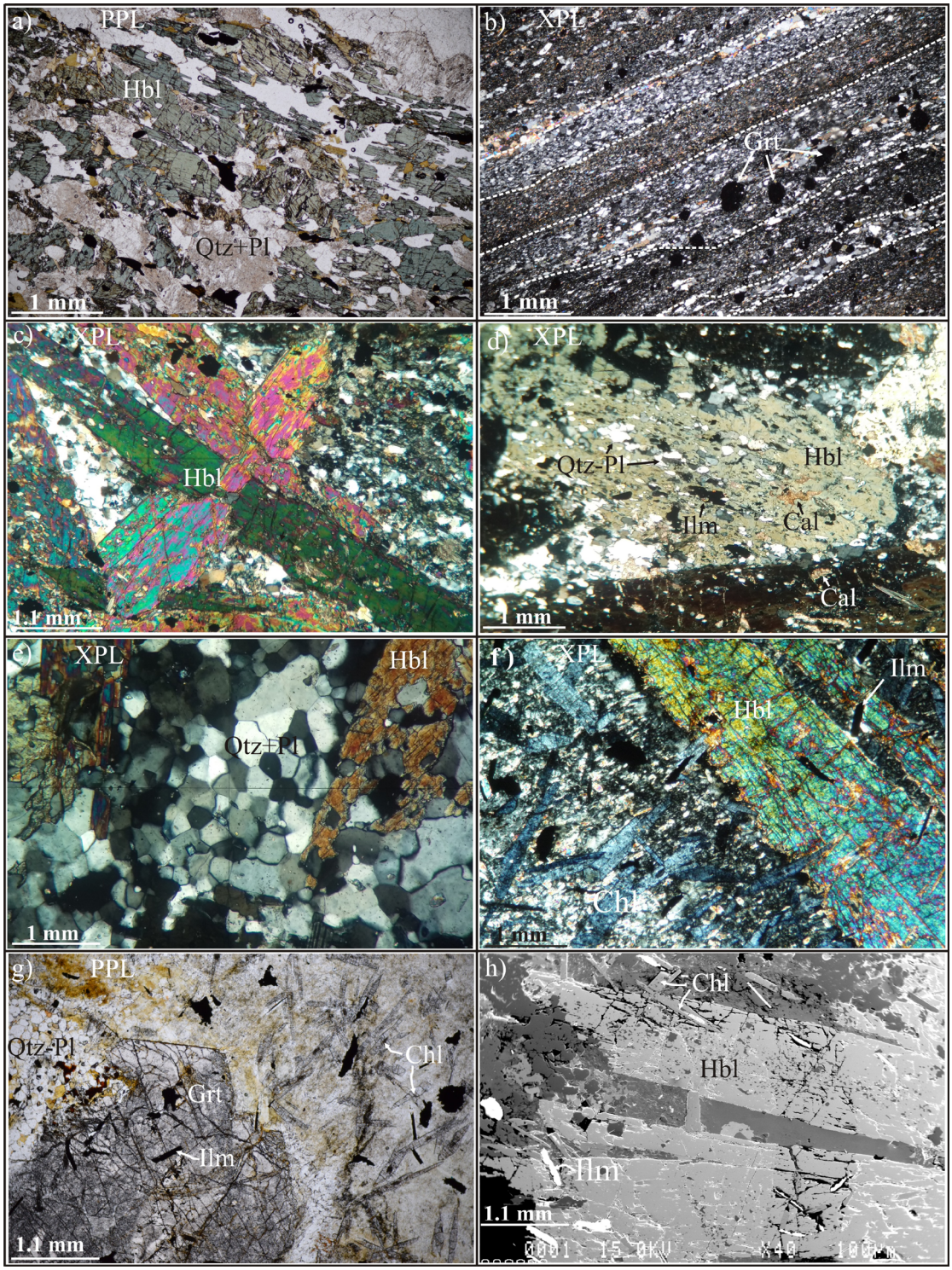

Figure 4. Photomicrographs of the studied metamorphic rock units, a: Orientation of hornblende and plagioclase porphyroblasts in amphibolites. b: Development of slaty cleavage parallel to primary bedding in the phyllites. c: Crosscutting hornblende porphyroblasts contain quartz, feldspar, and opaque inclusions. d: Microscopic image from oriented inclusions in the hornblende porphyroblasts. e: Recrystallized polygonal quartz-feldspars in the matrix of Garbenschiefer phyllites from the Gol-e-Gohar complex. f: Blue flakes of chlorite have grown both on the matrix and on the hornblende porphyroblasts. g: Garnet euhedralporphyroblasts with quartz-feldspar and opaque inclusions. h: Back scatter electron image of feather-like hornblende porphyroblasts and crosscutting chlorites from the Gol-e-Gohar complex. Abbreviations of mineral names are from Kretz (1983). Abbreviations: Hbl: hornblende; Amp: amphibole; Chl: Chlorite; Cal: calcite; Ep: epidote; Pl: plagioclase; Qtz: quartz; Grt: garnet; Ilm: ilmenite; Ttn: titanite (sphene) and U Rim: Upper Rim; Mid: Middle; L Rim: Lower Rim. Abbreviations of mineral names are from Kretz (1983).

grains show a mosaic, granoblastic texture, suggesting that these parts of the rock have been recrystallized under static conditions and their textures have changed into unoriented, coarse-grained ones (Figure 4e). Feather-shaped hornblendes consist of up to 30% of the rock volume. Chlorites in these rocks occur as two types. The first group is developed in the matrix as thin green- to dark green flakes with diameters up to 2 mm, representing a weak schistosity along with fine-grained muscovite. Another group occurs as blue blades (moderately 2 mm in length) grown on both schistosity and hornblende radial aggregates (Figure 4f) belonging to the next retrograde metamorphic event. The matrix consists of a fine-grained recrystallized granoblastic set of undeformed quartz and feldspars with a mosaic texture. Garnet porphyroblasts up to 20 mm in diameter occur as euhedral grains (Figure 4g) that contain quartz-feldspar inclusions and consist of only 5% of the rock volume. The existence of S1 internal foliation as inclined inclusion trails in these garnets suggests that they have been formed during regional metamorphism. Feldspars are seen either as oriented fine-grained inclusions in the hornblende porphyroblasts or unoriented mosaic shaped in the matrix. There are small amounts of hematite, calcite, titanite, and ilmenite (up to 2 vol.%) in these rocks (Figure 4h).

4.3. Mineral chemistry

4.3.1. Amphibole

Table 1 represents the chemical compositions of feather-shaped hornblendes from the Gol-e-Gohar metamorphic complex. As shown in Figure 5, they are ferro-pargasitic hornblende and ferro-tschermakite in composition (nomenclatures are from Leake et al., 1997). Figures 6a and 6b show an aggregate of the hornblendes in which crystals have grown from a point (shown as "core") toward the left and right. In order to investigate chemical variations along the C axes of these crystals, some points along the longitudinal lines (shown as 1, 2, and 3 in Figure 6b) were analyzed. Si contents increase from cores to the rims in the longitudinal profiles (Figure 6c). Mg average concentrations increase from the center to the rim and indicate a semilunar pattern. This semilunar pattern shows that the average Fe concentration in the studied hornblendes is oscillatory. Generally, in these profiles, Mg, Si, and Na cation concentrations increase and Fe, Al, and Ti decrease from the cores to the rims. In order to explore the chemical compositions of each crystal in the aggregate, a series of analyses were performed from the width of the crystals, presented as traverses 1–6 in Figure 7. The amounts of major elements in chemical profiles (Figure 7) indicate distinctive variations. Fe profile shows an upward convex and decreases from the upper crystal to the lower one. Average amounts of Mg increase toward the lower crystal, while Al, Na, and Ti average concentrations decrease (Figure 7). According to Leake et al. (1997), the amphiboles from Gol-e-Gohar metabasites fall in the field of tschermakite-hornblende. These amphiboles contain less than 0.2 p.f.u Ti in their structural formula and their amounts of Ti decrease slightly with increasing of Al^{IV} values. This reduction of Ti can be related to increasing Si amounts in the crystals. Presence of minerals such as sphene, magnetite, ilmenite, and quartz along with amphibole in the metabasites suggests high oxygen fugacity conditions during crystallization of the studied amphiboles.

4.3.2. Garnet

Representative chemical analyses of the studied garnets (Table 2) show that they contain almandine (0.66–0.70), grossular (0.18–0.22), spessartine (0.04–0.05), and pyrope (0.05–0.08). The X_{Fe} (Fe/(Fe + Mg)) ratio is high and ranges between 0.88 and 0.92. In combinational profiles (Figure 8), pyrope content increases from their centers to the rims. The almandine component shows negligible changes from the center to the rim, but grossular and spessartine profiles show decreasing trends from the center to the rim.

4.3.3. Epidote

Representative analyses of epidotes in the studied rocks are shown in Table 2, with their structural formula calculated based on 12.5 oxygen. Chemical compositions of these minerals from their cores to the rims show little variations so that Al_2O_3 ranges between 28.67 and 29.88 wt.% and the contents of pistacite end-member (Xps= $Fe^{3+}/Al+Fe^{3+}$) change between 10.66 and 12.14.

4.3.4. Chlorite

In Table 2, some analyses of chlorite needles in the studied rocks are shown. They are ripidolite in composition (Hey, 1954) (Figure 9) and formed after the formation of feather-shaped hornblendes and developed randomly throughout the studied rocks. The average concentrations of Al, Fe, and Mg cations are 5.5, 4.25, and 4.8 p.f.u., respectively. Therefore, Fe decreases from the center to the rim. Moreover, average amounts of Mg increase from the center to the rim.

4.3.5. Feldspars

Chemical analyses of the feldspars from the studied rocks are shown in Table 2. Chemically, they are divided into two groups. In the first group, An contents vary between 23 and 25 and therefore they are oligoclase in composition. Under the microscope, this group occurs as fine-grained but the second group is andesine considering the average contents of their An, which is 40. The latter appears as coarse-grained in the rocks. The average content in the plagioclases decreases from 41.5 in the cores to 25 in the rims, suggesting a temperature drop during crystallization of these minerals (Stokes et al., 2012).

Table 1. Representative analyses of hornblendes in the studied phyllites.

Rock type	Phyllite											
Phase	Amphibole (Traverse 2)						Amphibole (Traverse 3)					
	U Rim	U Rim	Mid	Mid	L Rim	L Rim	U Rim	U Rim	Mid	Mid	L Rim	L Rim
SiO_2 (wt%)	41.44	41.97	42.14	42.07	42.17	41.74	42.29	41.76	41.92	42.48	42.25	42.68
TiO_2	0.32	0.26	0.24	0.45	0.27	0.27	0.31	0.28	0.25	0.23	0.28	0.26
Al_2O_3	19.90	19.92	20.34	19.89	19.92	19.99	20.21	20.56	20.47	20.38	19.99	20.29
FeO	16.99	17.30	17.27	18.55	17.28	17.38	17.40	17.90	18.29	18.27	17.85	17.29
MnO	0.09	0.15	0.14	0.15	0.07	0.21	0.16	0.18	0.18	0.09	0.14	0.15
MgO	5.90	5.76	5.63	5.40	5.90	5.98	6.04	5.39	5.55	5.81	5.72	5.92
CaO	11.49	11.29	11.53	11.36	11.53	11.21	11.46	11.38	11.35	11.53	11.32	11.43
Na_2O	1.29	1.39	1.23	1.31	1.23	1.30	1.44	1.20	1.22	1.39	1.24	1.45
K_2O	0.52	0.45	0.44	0.42	0.44	0.40	0.49	0.44	0.39	0.45	0.42	0.50
F	0.04	0.01	0.26	0.07	0.23	0.11	0.24	0.19	0.22	0.27	0.00	0.20
Cl	0.02	0.01	0.00	0.01	0.00	0.00	0.01	0.01	0.00	0.00	0.01	0.00
Total	98.00	98.51	99.22	99.68	99.04	98.59	100.05	99.29	99.84	100.90	99.22	100.17
Formula	23 O											
Si	6.106	6.143	6.138	6.109	6.149	6.087	6.105	6.075	6.058	6.089	6.130	6.151
Ti	0.035	0.029	0.026	0.049	0.030	0.030	0.034	0.031	0.027	0.025	0.030	0.029
Al^{iv}	1.894	1.857	1.862	1.891	1.851	1.913	1.895	1.925	1.942	1.912	1.870	1.849
Al^{vi}	1.563	1.579	1.630	1.512	1.572	1.524	1.545	1.601	1.545	1.532	1.549	1.598
Fe^{3+}	0.160	0.200	0.147	0.297	0.180	0.384	0.241	0.296	0.410	0.318	0.314	0.166
Fe^{2+}	1.934	1.918	1.957	1.955	1.927	1.736	1.861	1.882	1.800	1.872	1.852	1.918
Mn	0.011	0.018	0.018	0.018	0.009	0.025	0.020	0.022	0.022	0.011	0.018	0.018
Mg	1.296	1.256	1.223	1.168	1.283	1.300	1.300	1.168	1.196	1.241	1.238	1.271
Ca	1.813	1.770	1.800	1.768	1.802	1.752	1.773	1.773	1.758	1.771	1.760	1.765
Na	0.370	0.394	0.349	0.370	0.348	0.367	0.404	0.338	0.343	0.387	0.348	0.405
K	0.098	0.084	0.081	0.078	0.081	0.074	0.090	0.081	0.073	0.082	0.078	0.092
F	0.017	0.005	0.122	0.034	0.105	0.050	0.108	0.086	0.102	0.125	0.000	0.091
Cl	0.004	0.003	0.000	0.003	0.000	0.000	0.003	0.002	0.000	0.001	0.001	0.000
Total	15.30	15.25	15.35	15.25	15.33	15.24	15.37	15.28	15.27	15.36	15.18	15.353
$Mg/(Mg + Fe^{2+})$	0.401	0.396	0.385	0.374	0.400	0.428	0.411	0.383	0.399	0.399	0.401	0.399

4.3.6. Muscovite

As shown in Table 2, analyzed muscovite contains a considerable amount of paragonite constituent and a small amount of phengite component. Fe, Mg, K, and Na average concentrations are 0.07, 0.07–0.1, 0.62, and 0.07–0.12, respectively. Moreover, Na/(K+Na) ratio changes between 0.07 and 0.15. In the studied muscovites, with increasing calculated temperatures, Na_2O content increases while FeO, MgO, and SiO_2 decrease. This is consistent with other studied areas in the world (Graessner and Schenk, 1999).

4.3.7. Ilmenite

In the studied rocks, ilmenite occurs as small needles with an aspect ratio of 4:1 and 1 mm in length and is distributed randomly in the matrix. As shown in Table 2, TiO_2 and FeO_t contents are 48.47–53.6 and 37.7–45.9 wt.%, respectively.

4.4. Thermometry

Petrographic features revealed that the primary mineral assemblage of the studied rocks was plagioclase, chlorite, quartz, and muscovite and probably pyroxene. In addition, after fluid/rock interaction and formation of feather-

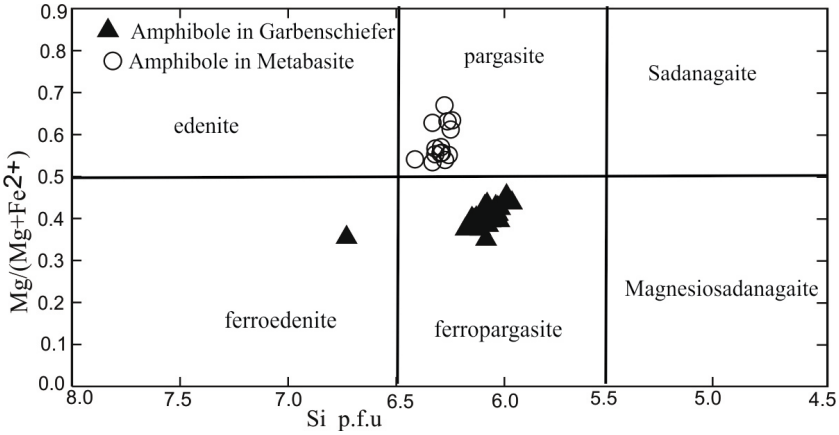

Figure 5. Chemical compositions of amphiboles from the Gol-e-Goharmetabasites (open circles) and those which have crystallized in the Gol-e-GoharGarbenschiefer phyllites (solid triangles). Namenclatures are from Leake et al. (1997). Amphibole formula calculated following Holland and Blundy (1994).

shaped hornblendes coexisting minerals are amphibole, garnet, plagioclase, quartz, and ilmenite. Textural evidence such as straight boundaries between the hornblendes and plagioclases and the lack of replacement features between them (Figure 4e) shows that they are in equilibrium. Accordingly, to calculate the thermal conditions for the formation of chlorite and hornblende aggregates in phyllites, we use the hornblende-plagioclase thermometer (Holland and Blundy, 1994) and chlorite thermometry (Cathelineau and Nieva, 1985). The hornblende-plagioclase thermometer of Holland and Blundy (1994) is applicable in the P-T range 400–1000 °C and 1–15 Kbar on a broad range of bulk composition and is based on two reactions involving amphibole and plagioclase end members:

Edenite + Quartz = Tremolite + Albite (1)

Edenite + Albite = Richterite + Anorthite (2)

We use reaction (1) and a pressure of 5 kb for calculating the temperature conditions of the studied samples. The sensitivity of this thermometer to plagioclase contents is minimal. To calculate metamorphic conditions, we used chemical compositions of the cores and rims of both amphibole and plagioclase. Calculated temperatures are 535 °C in the cores and 490–505 °C in the rims, indicating a temperature drop of about 30 °C during crystallization of the minerals. Decreasing temperature during crystallization is characterized by decreases in both Al and Ti contents of amphibole and An contents of plagioclase from their cores to the rims. Temperature rise during the formation of amphibole causes increasing Al^{IV} and Ti contents (Hammarstorm and Zen, 1986). In the studied amphiboles, Al^{IV} and Ti contents slightly decrease from their cores to the rims, which correspond to the temperature reduction during crystallization. Moreover, chlorite thermometry (Cathelineau and Nieva, 1985) based on T = 213.3 Al^{IV} + 17.5 indicates temperatures of 308–315 °C for the formation of the studied chlorite needles. However, as Topus (2006) demonstrated for contact metamorphism around the Eocene Saraycık granodiorite, Eastern Pontides, Turkey, when fluids are involved in contact metamorphic processes, all primitive relations change and disequilibrium textures appear due to variations in temperature and fluid composition. In the studied rocks, the calculated P-T information is attributed to the fluid dominated conditions during contact metamorphism, not to the pre-contact metamorphic assemblages.

5. Discussion

In hydrothermal metamorphism (Coombs, 1961), hot aqueous solutions or gases flow through fractured rocks and cause some mineralogical and chemical changes in them. This wall–rock interaction occurs at all temperatures from the surface to very hot conditions above 200 °C. There is a line of evidence that suggests the studied feather-shaped hornblendes and the Gol-e-Gohar Garbenschiefer phyllites have been formed by hydrothermal metamorphism. Through the field survey, several fractures are observed in the phyllites along which many hornblende needles have developed outward and arranged almost normal to the fracture planes (Figures 10a and 10b). This feature suggests that the hornblendes have been formed from hydrothermal fluids ascending via the fractures. On a microscopic scale, undeformed hornblende porphyroblasts have overprinted the former schistosity. Moreover, the absence of deflection of S_e, lack of strain shadows, and undulose extinction suggest that these porphyroblasts grew after a pervasive schistosity in

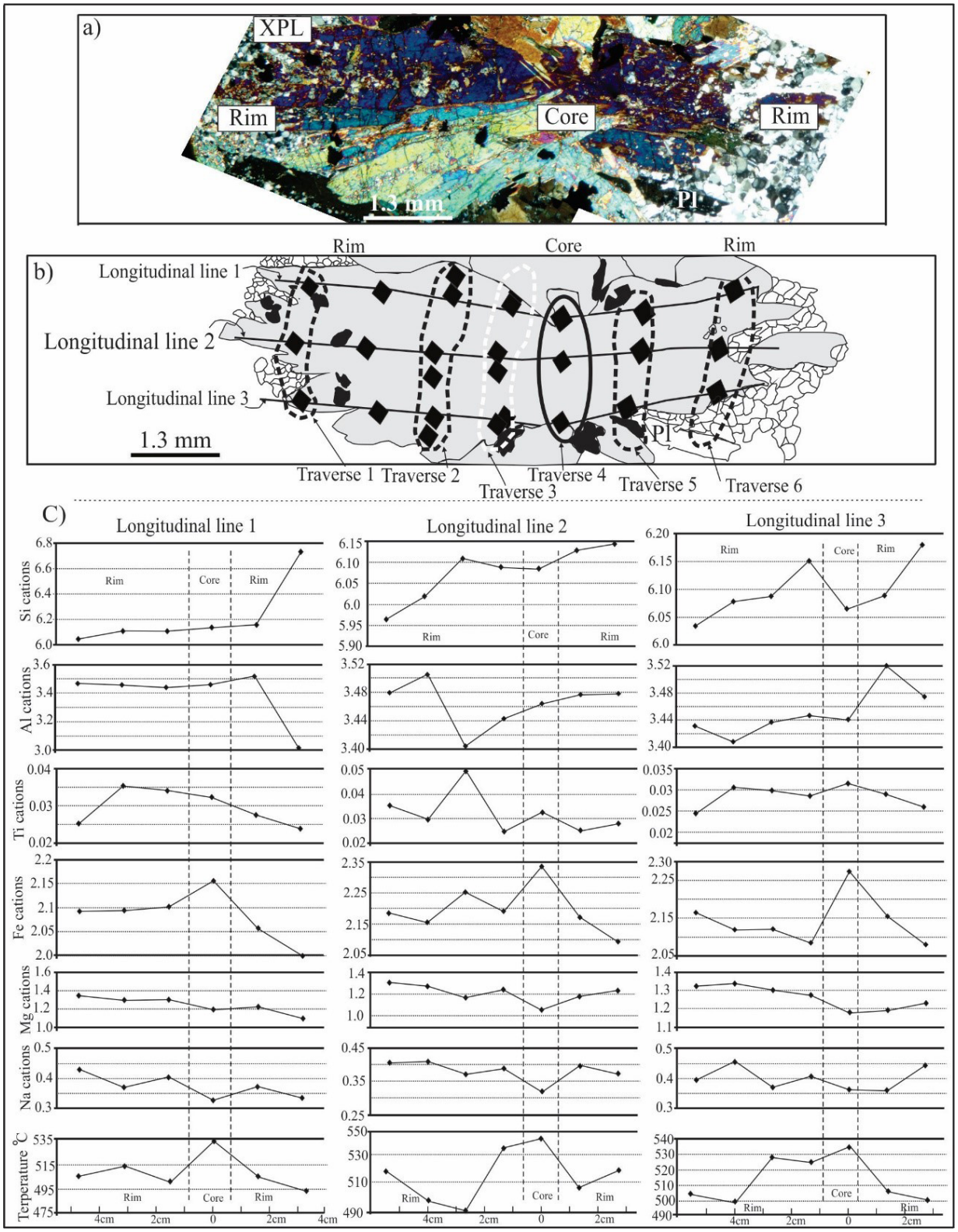

Figure 6. a: Photomicrograph of analyzed a radial hornblende aggregate. These hornblendes have grown from a point (shown as "core") to the left and right. b: This figure is a drawing of figure (a) as a whole on which analyzed points are shown. c: Chemical longitudinal variations of hornblende compositions that have delineated along the C axes of the crystals.

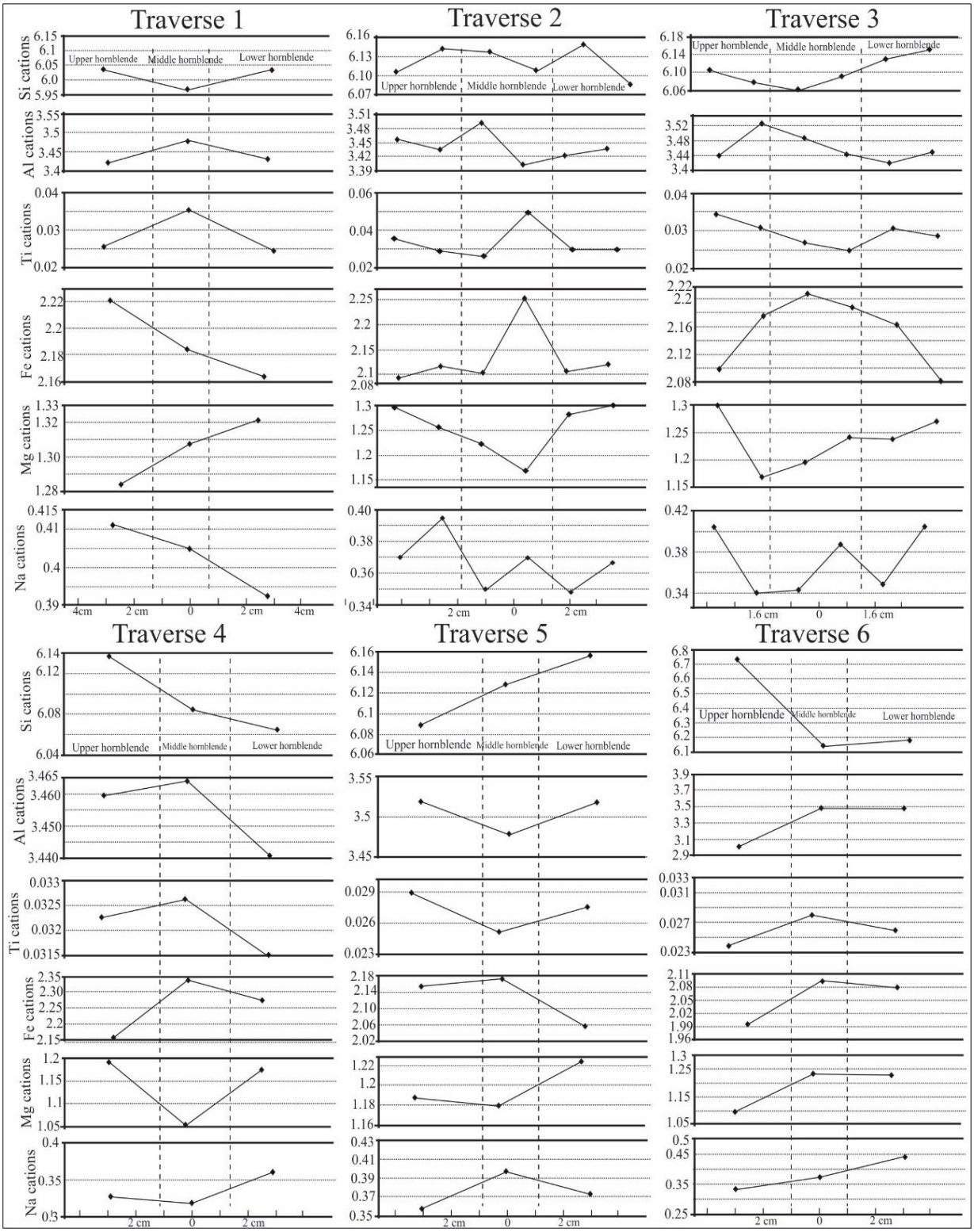

Figure 7. Traverses 1–6 show chemical variations in hornblendes from aggregate in Figure 6a. These diagrams (called traverses) are delineated from the upper hornblende crystal toward the lower crystal.

Table 2. Representative analyses of the main phases in the studied phyllites.

Rock type	Phyllite													
Phase	Grt			Pl			Chl		Ep		Ms		Ilm	
	Core	Mid	Rim	Rim	Core	Core								
SiO_2 (wt%)	38.23	38.27	38.45	62.36	58.46	61.80	25.17	25.42	38.73	38.90	46.58	46.61	0.69	0.00
TiO_2	0.13	0.09	0.02	0.02	0.00	0.00	0.03	0.08	0.09	0.16	0.27	0.26	48.47	48.57
Al_2O_3	21.30	21.46	21.70	23.72	26.66	26.32	22.19	22.41	29.22	28.67	34.53	35.53	0.76	0.02
FeO	29.93	30.82	31.32	0.00	0.01	0.14	24.61	23.89	4.91	5.41	1.55	1.33	44.76	44.94
MnO	1.89	1.94	2.20	0.10	0.05	0.00	0.02	0.07	0.03	0.02	0.00	0.00	0.95	0.96
MgO	1.70	1.35	2.18	0.01	0.00	0.01	15.72	15.73	0.02	0.04	1.08	0.87	0.23	0.06
CaO	7.58	6.89	6.66	5.18	8.54	7.99	0.03	0.00	24.00	24.04	0.22	0.38	0.03	0.04
Na_2O	0.04	0.01	0.00	8.69	6.66	6.63	0.00	0.03	0.04	0.00	0.82	1.01	0.10	0.00
K_2O	0.01	0.00	0.01	0.03	0.04	0.04	0.00	0.00	0.01	0.01	9.23	8.85	0.02	0.00
Cl	0.00	0.00	0.02	0.00	0.01	0.00	0.00	0.13	0.00	0.14	0.00	0.00	0.00	0.01
F	0.00	0.00	0.00	0.07	0.02	0.06	0.05	0.08	0.01	0.01	0.00	0.00	0.35	0.00
Total	100.82	100.84	102.56	100.18	100.46	102.99	87.83	87.84	97.06	97.41	94.27	94.84	96.35	94.61
Formula	12 O			8 O			28 O		12.5 O		11 O		6 O	
Si	3.036	3.047	3.001	2.762	2.600	2.668	5.260	5.277	3.003	3.014	3.116	3.090	0.036	0.000
Ti	0.008	0.006	0.001	0.001	0.000	0.000	0.004	0.013	0.005	0.009	0.014	0.013	1.894	1.941
Al	1.993	2.014	1.996	1.238	1.398	1.339	5.473	5.504	2.670	2.618	2.723	2.777	0.046	0.001
Cr	0.001	0.003	0.002	0.000	0.000	0.000								
Fe^{3+}	0.000	0.000	0.000	0.000	0.000	0.004	0.028	0.107	0.318	0.351	0.000	0.000	0.076	0.106
Fe^{2+}	1.988	2.052	2.044	0.000	0.000	0.000	4.274	4.040			0.087	0.074	1.869	1.891
Mn	0.127	0.131	0.145	0.004	0.002	0.000	0.004	0.012	0.002	0.001	0.000	0.000	0.042	0.043
Mg	0.201	0.160	0.254	0.000	0.000	0.001	4.897	4.868	0.002	0.005	0.108	0.086	0.017	0.005
Ca	0.645	0.588	0.557	0.248	0.423	0.431	0.007	0.000	1.994	1.995	0.016	0.027	0.002	0.002
Na				0.747	0.574	0.555	0.000	0.023	0.007	0.000	0.106	0.129	0.010	0.000
K				0.002	0.002	0.002	0.002	0.000	0.001	0.001	0.787	0.748	0.001	0.000
Cl							0.000	0.090			0.000	0.001		
F							0.069	0.104			0.000	0.000		
Total	8.00	8.00	8.00	5.00	5.00	5.00	20.01	20.03	8.00	7.99	6.95	6.94	3.99	3.99
X_{alm}	0.671	0.700	0.681											
X_{prp}	0.068	0.055	0.085											
X_{grs}	0.218	0.201	0.186											
X_{spes}	0.043	0.045	0.048											
X_{Fe}	0.908	0.928	0.890											
Ab				75.101	58.368	59.886								
An				24.724	41.380	39.876								
Or				0.175	0.252	0.238								

Abbreviations: Chl: Chlorite; Ep: epidote; Pl: plagioclase; Grt: garnet; Ilm: ilmenite; Mid: Middle; Xalm: almandine proportion, Xprp: pyrope proportion, Xgrs: grossular proportion, Xspes: spessartine proportion, X_{Fe}: $Fe/(Fe + Mg^{2+})$; An: anorthite; Ab: albite; Or: orthoclase.

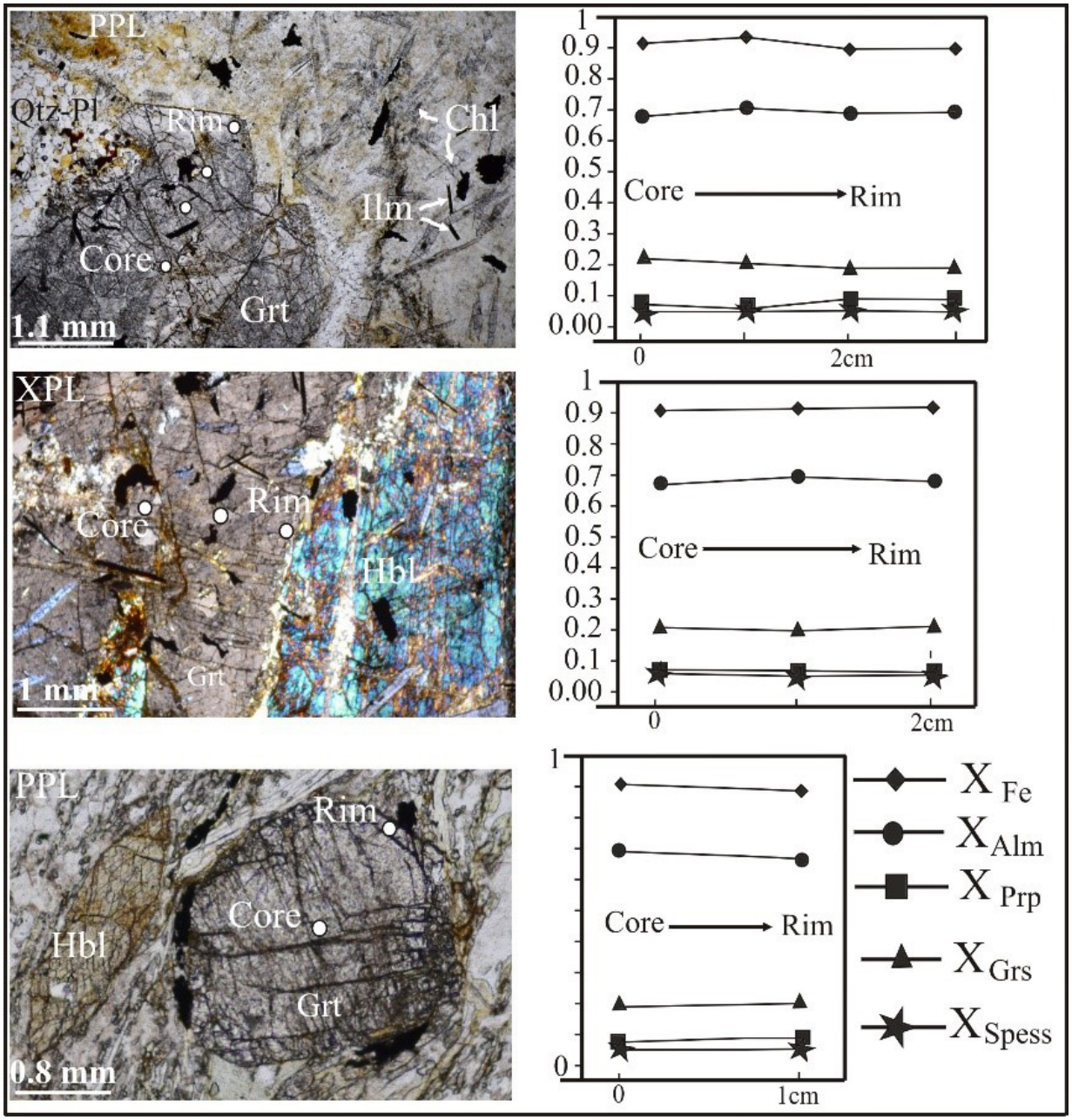

Figure 8. Compositional variations of garnets in the studied phyllites.

static conditions. Moreover, quartz-feldspar inclusions within these crystals show strong orientation; however, the same minerals between the hornblendes in the matrix show mosaic textures without any orientation, suggesting that the matrix has been affected by static recrystallization processes. Such a feature can be formed by fluid-rock interaction and re-equilibration of the grains (Springer and Day, 2002).

Chemically, there are differences between chemical compositions of hydrothermal derived hornblendes with those formed by progressive metamorphism. As Springer and Day (2002) stated, hydrothermal amphiboles (magnesi-ohornblende, ferro-hornblende, tschermakite, barroisite and ferro-barroisite) can be distinguished from more typical very low-grade regional/contact amphiboles on the basis of composition if the formula unit is subcalcic (Ca < 1.9; Na > 0.1 p.f.u), aluminous (Si < 7.7; Al > 0.4 p.f.u), and/or titaniferous (Ti > 0.02 p.f.u). According to Silantyev et al. (2008), subcalcic and low-Ti amphiboles are more commonly associated with high-temperature

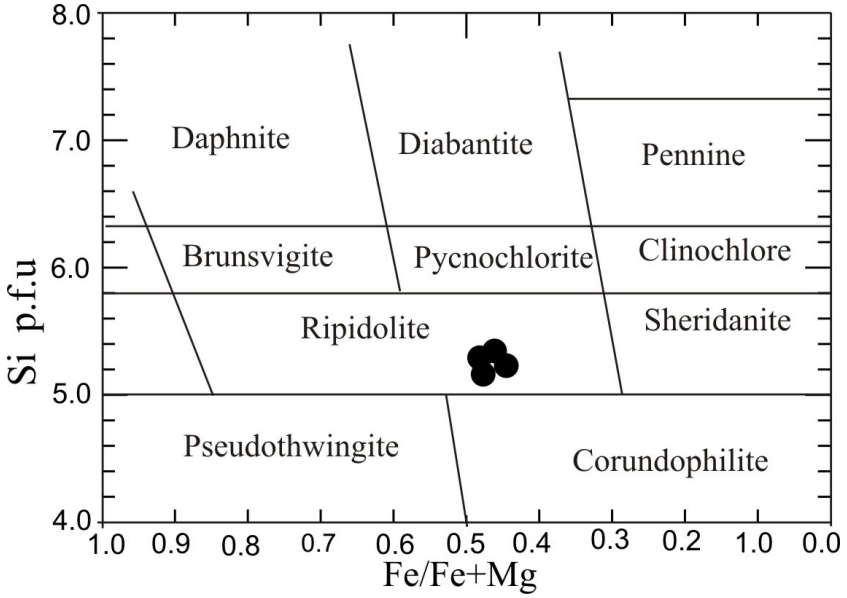

Figure 9. Classification of chlorites based on Hey (1954). Chlorites are ripidolite in composition.

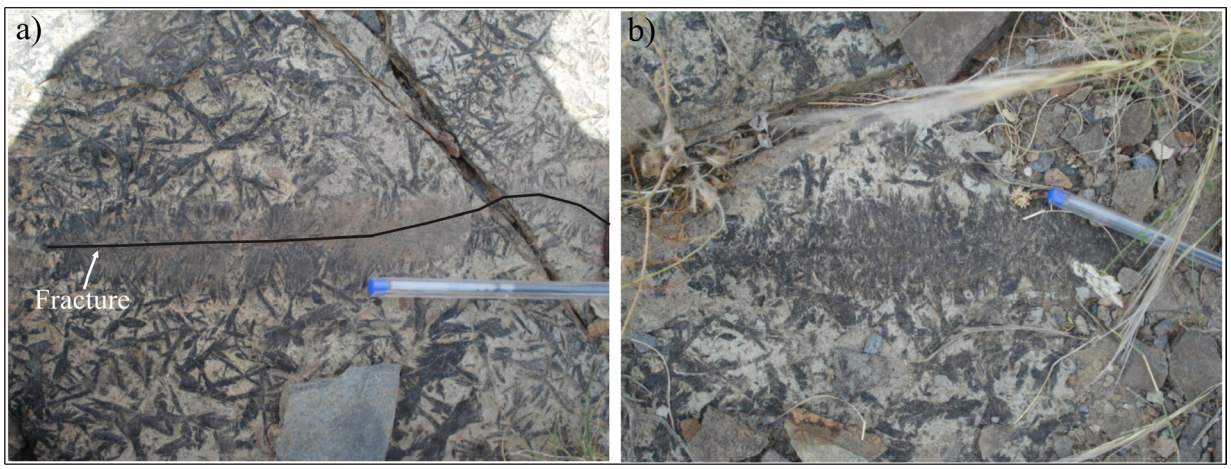

Figure 10. a and b: Two outcrops show concentrations of hornblende needles around the fractures in the phyllites of the Gol-e-Gohar complex.

hydrothermal metamorphism. The studied amphiboles from the Gol-e-Gohar complex are subcalcic (Ca is less than 1.9 and Na is more than 0.1 p.f.u.) and the amounts of Ti change between 0.03 and 0.2 p.f.u. Therefore, their compositions are consistent with the formation during hydrothermal metamorphism. Furthermore, there are many amphiboles in the Gol-e-Gohar metabasites (these rocks are shown in Figure 2 as metabasaltic lava flows or amphibole-schists). Chemical compositions of these amphiboles are completely different from those existing in the hornblende aggregates of the phyllites (Figure 11). As shown in Table 3, amphiboles of the amphibole-schists (Metabasites) have Ca < 1.75, Na > 0.4, and Ti > 0.07 p.f.u; thus, according to Springer and Day (2002), they are classified as metamorphic hornblendes. Other studies (e.g., Silantyev et al., 2008) demonstrated that subcalcic and low-Ti amphiboles are more commonly associated with high-temperature hydrothermal metamorphism. Chemically, the formation of hornblende was accompanied by gains in Mg and Fe and losses in K and Na. Thus, hornblende-rich phyllites in the studied rocks could correspond to the interaction of Mg-Fe rich fluids with quartz-feldspathic rocks. Chemical variations in the hornblendes from their cores to the rims suggest drastic changes in the fluid

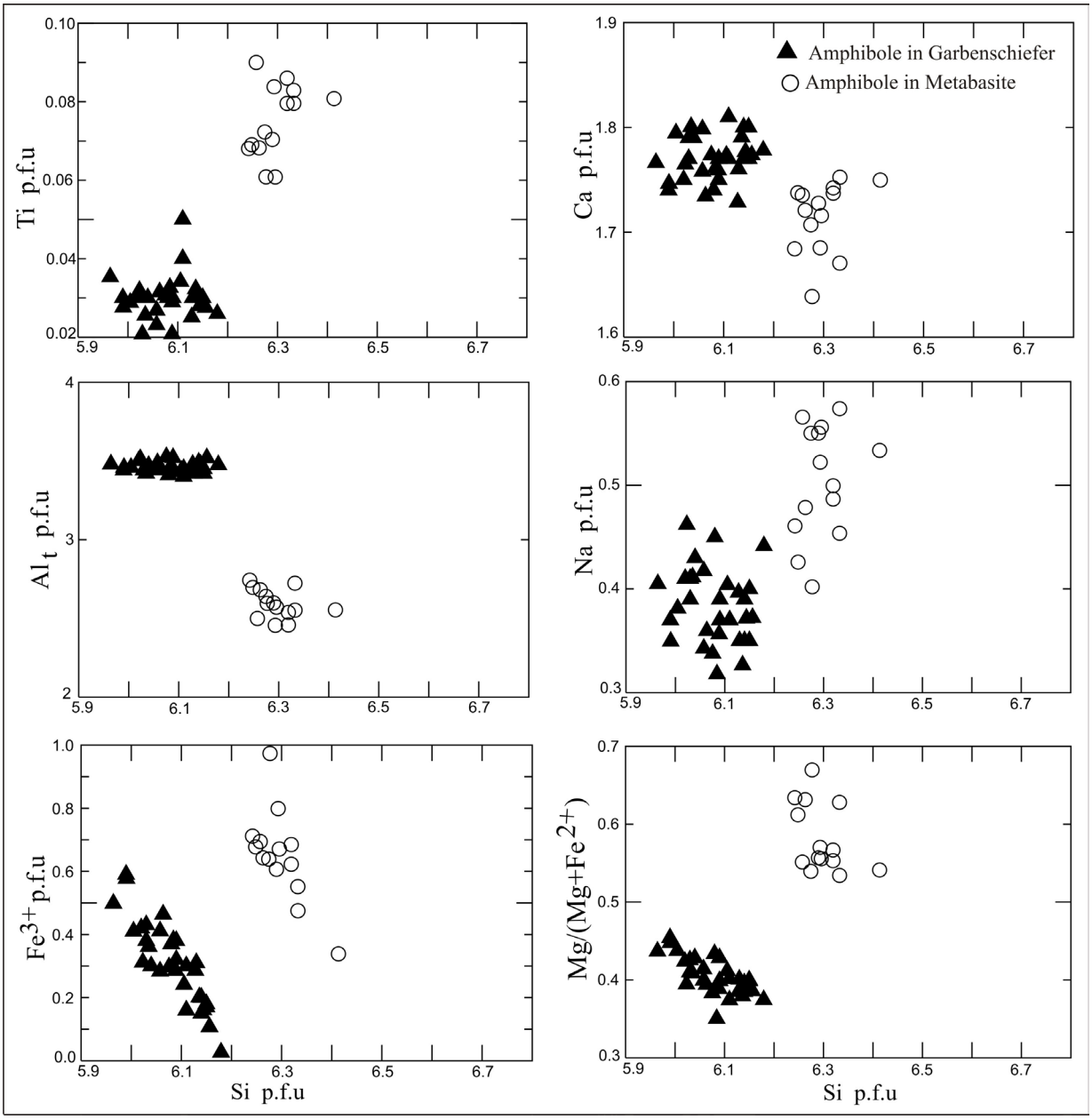

Figure 11. Comparison between the chemical compositions of amphiboles in metabasites and those that exist in the hornblende aggregates of the phyllites.

composition from which the hornblendes have been crystallized. The variation in the fluid composition can be attributed to the movement of fluids along gradients in pressure and temperature (Hemley et al., 1971). Fluid flow along positive temperature gradients would favor fixation of Ca or Mg (Rose and Bird, 1994). In contrast, losses in Ca and gains in K and Na are explained as the result of fluid flow in the direction of a temperature drop (Streit and Cox, 1998). In the case of phyllite from the Gol-e-Gohar complex, longitudinal chemical profiles (Figure 6) show that, in the fluid, elements such as Mg, Si, and Na increased while Fe, Al, and Ti decreased during crystallization of the hornblende needles, suggesting that the fluid flowed in the temperature drop direction. However, Hacker et al. (2003) showed that the amphiboles could form under conditions of high-temperature (>300 °C) interaction of hydrous fluids within the rocks.

Different parts of the hornblende blades show chemical variations suggesting that Mg and Fe acted as mobile elements, while Al and Ti were immobile during

Table 3. Representative analyses of hornblendes in the studied metabasites.

Rock type	Metabasite											
Phase	Hornblendes											
SiO_2 (wt%)	43.19	42.96	43.54	43.37	42.65	43.92	43.44	43.48	43.37	42.94	42.77	43.03
TiO_2	0.76	0.82	0.79	0.65	0.55	0.64	0.73	0.73	0.56	0.66	0.71	0.64
Al_2O_3	14.30	14.56	14.37	15.54	15.78	16.37	14.80	14.69	15.03	15.33	14.62	15.08
FeO	18.35	18.36	17.91	15.81	16.33	15.93	17.70	16.14	17.95	17.90	17.16	17.32
MnO	0.07	0.12	0.10	0.14	0.08	0.05	0.07	0.06	0.05	0.10	0.13	0.11
MgO	8.78	8.72	9.00	9.69	8.98	9.66	8.74	8.86	8.71	8.33	8.57	8.71
CaO	10.79	11.12	11.17	11.04	11.11	11.06	11.18	11.07	11.03	10.90	11.05	11.03
Na_2O	1.85	2.00	1.77	1.63	1.56	1.67	1.73	1.87	1.98	1.94	2.00	1.94
K_2O	0.45	0.36	0.38	0.44	0.48	0.52	0.35	0.43	0.30	0.34	0.36	0.30
F	0.23	0.00	0.00	0.00	0.13	0.00	0.13	0.00	0.04	0.02	0.08	0.31
Cl	0.03	0.10	0.06	0.05	0.04	0.07	0.04	0.01	0.03	0.07	0.04	0.02
Total	98.80	99.12	99.09	98.36	97.69	99.89	98.90	97.35	99.04	98.53	97.50	98.49
Formula	23 O											
Si	6.293	6.257	6.319	6.266	6.246	6.242	6.319	6.413	6.296	6.274	6.332	6.290
Ti	0.080	0.090	0.086	0.071	0.061	0.068	0.080	0.081	0.061	0.072	0.080	0.070
Al^{iv}	1.710	1.743	1.681	1.734	1.754	1.758	1.681	1.587	1.704	1.726	1.668	1.710
$Al\ v^{i}$	0.750	0.756	0.778	0.912	0.968	0.985	0.857	0.967	0.866	0.914	0.885	0.888
Fe^{3+}	0.800	0.694	0.685	0.722	0.646	0.712	0.623	0.339	0.671	0.639	0.475	0.607
Fe^{2+}	1.440	1.542	1.490	1.188	1.354	1.182	1.532	1.653	1.508	1.549	1.650	1.510
Mn	0.010	0.014	0.013	0.017	0.010	0.006	0.009	0.007	0.006	0.012	0.016	0.013
Mg	1.910	1.894	1.948	2.087	1.960	2.046	1.895	1.949	1.885	1.814	1.892	1.898
Ca	1.690	1.735	1.737	1.709	1.742	1.684	1.742	1.750	1.716	1.707	1.752	1.728
Na	0.520	0.566	0.500	0.457	0.444	0.461	0.487	0.534	0.556	0.550	0.574	0.550
K	0.080	0.066	0.071	0.081	0.089	0.095	0.065	0.082	0.055	0.064	0.068	0.056
F	0.105	0.000	0.000	0.000	0.058	0.000	0.058	0.000	0.019	0.010	0.039	0.144
Cl	0.008	0.025	0.014	0.011	0.010	0.017	0.010	0.003	0.007	0.017	0.009	0.005
Total	15.397	15.383	15.321	15.255	15.344	15.255	15.357	15.364	15.350	15.348	15.441	15.468
$Mg/(Mg + Fe^{2+})$	0.570	0.551	0.567	0.637	0.592	0.634	0.553	0.541	0.555	0.539	0.534	0.557

hydrothermal metamorphism. As Essaifi et al. (2004) showed, the behavior of elements in hydrothermal systems is controlled by the chemical composition of infiltrating fluid, direction of fluid flow, and the nature of fluid flux along the shear zones. Ca and Mg were fixed in up-temperature flow zones and leached in down-temperature up zones. Na was leached in all the shear zones, probably as a result of the high fluid fluxes.

According to Steffen et al. (2014), in the Greiner shear zone of the Alps, similar rocks were formed via a succession of weakening and strengthening episodes. As they stated, in the first stage, a grain-size reduction due to grain boundary diffusion creep (GBDC) occurred and fine-grained plagioclase-rich horizons were produced. This mechanism promotes the strain rate in these horizons relative to adjacent layers. In the second stage, rapid diffusion rates due to GBDC result in rapid growth of large crosscutting hornblende crystals, while in the third stage reaction-induced weakening occurs. In addition to the mechanisms proposed by Steffen et al. (2014) for the formation of similar rocks in the Greiner shear zone of the Alps, it seems that in the case of Gol-e-Gohar phyllites another factor also controlled the formation and the arrangements of the hornblendes. In these phyllites, there are many fractures along which spectacular arrays of hornblendes were developed (Figures 10 and 12),

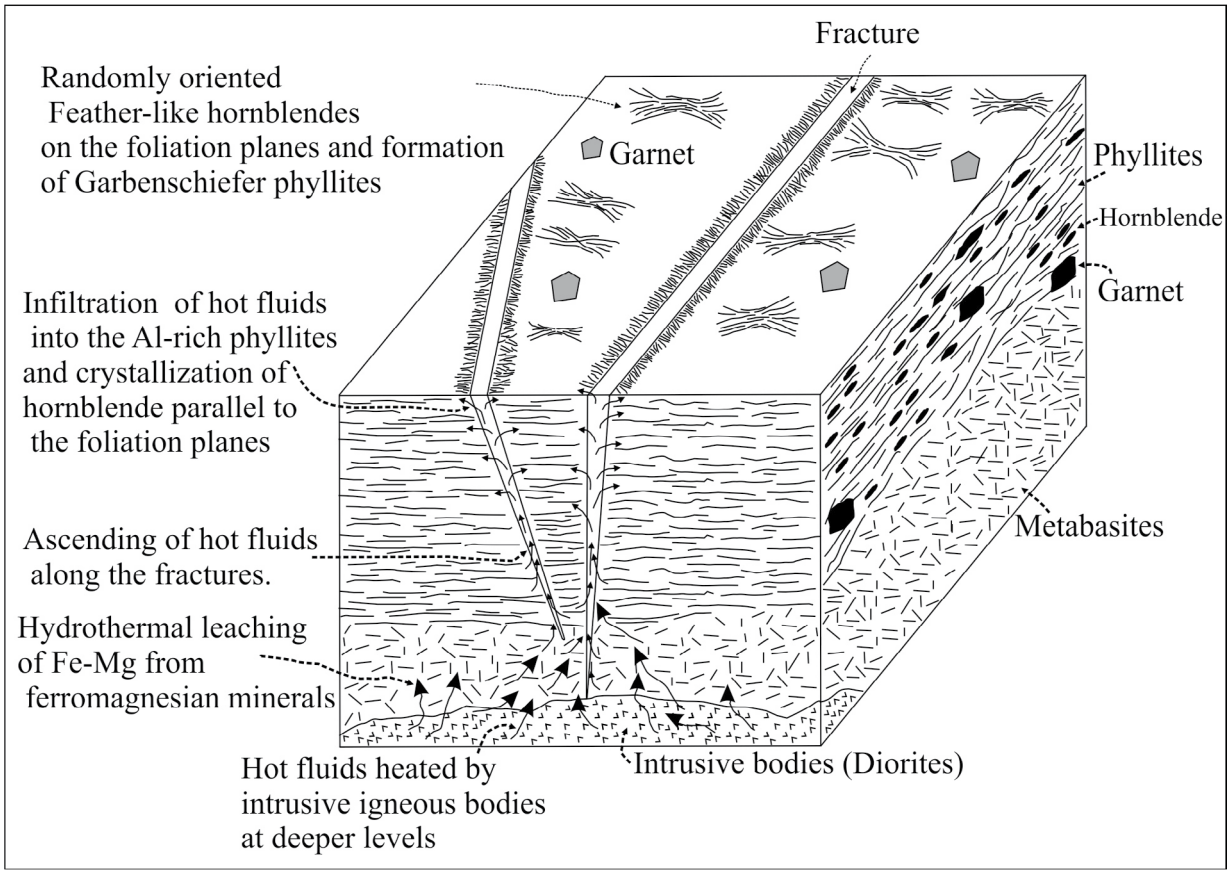

Figure 12. Schematic illustration summarizing the formation of feather-like hornblende aggregates in the Gol-e-Gohar complex.

suggesting that the fractures conduct the fluids and control the shapes and distribution of the hornblende aggregates. In the gabbroic rocks from Hess Deep, Kelley and Malpas (1996) showed that migration of the magmatic fluids along the fractures has led to the formation of greenschist facies mineral assemblages in gabbroic rocks. This process is most intense in parts adjacent to veins and in cataclastically deformed zones, wherein fractures enhanced fluid flow.

Several authors (Bevins and Robinson, 1994; Alt, 1999; Springer and Day, 2002; Essaifi, 2004) state that hydrothermal metamorphism occurs by fluid infiltration in shear zones. In the studied area, field evidence shows that the emplacement of dioritic and granitic intrusions causes thermal events. Distribution of major faults (Figure 1) suggests that the area has been tectonically active and shear zones could penetrate into the deeper levels of the crust, facilitating an ascendance of intrusion-derived hot fluids. Hence, in the case reported here, hydrothermal fluids could have moved up, interacted with the wall rock, and then precipitated the hornblende aggregates. Hydrothermal metamorphism mainly occurs in basaltic rocks of the seafloor (Alt, 1999). In this type of metamorphism, various mineral assemblage reflects variations in the temperatures and compositions of the circulating fluids with time and depth as well as the high geothermal gradients (>100 °C/km). However, this process can occur also in other geological environments such as the volcanic/sedimentary rocks from the convergent plate margins (Essaifi et al., 2004). By the development of amphibole-rich rocks, as the first nucleated shear zones evolved, the increased permeability allowed more fluids to infiltrate the shear zones and those that continued to undergo fluid infiltration were retrogressed into chlorite-rich mylonites (Essaifi et al., 2004). In the studied rocks from the Gol-e-Gohar complex, chlorite needles may have been formed during such retrograde metamorphism.

Garnet porphyroblasts in the studied rocks have two distinct occurrences. Inclusion patterns show that their centers have been formed during the formation of pervasive schistosity in the phyllites and therefore these parts are syntectonic. On the other hand, garnets have euhedral margins that can be produced by the reaction between plagioclase and amphibole grains in static conditions. Increasing Ca contents in hornblendes along with decreasing Ca and An contents in garnets from their centers to the margins suggest that the garnets probably

formed by reaction between hornblende and plagioclase as the following reaction (Kruse and Stunitz, 1999; Stokes et al., 2012):

Hornblende + Anorthite = Garnet + Quartz + H_2O (3)

Considering all the evidence, the following scenario can be stated for the formation of feather-textured hornblende aggregates in the Gol-e-Gohar complex. In the first stage, shearing forces resulted in a fine-grained matrix in which minerals show strong lattice-preferred orientation and a mylonite formed. Nowadays, the relics of that mylonite remain as small oriented deformed quartz and feldspar inclusions in hornblende porphyroblasts. In this stage, mechanisms such as GBCD could have acted in order to facilitate deformation processes. GBCD is a grain-size sensitive process requiring rapid intercrystalline diffusion. This high diffusion rate may result from deformation-enhanced fluid distribution (Tullis et al., 1996). All the hornblendes studied in the present work are strain-free and there is no deformational evidence in them. Thus, we inferred that they have been crystallized under static conditions when GBDC ceased.

Fluids ascended from the deeper levels of the shear zone into the phyllites and distributed laterally along the foliation surfaces. These infiltrated fluids resulted in the formation of hornblende aggregates between highly deformed mylonitic phyllites. Formation of hornblendes along with garnets and recrystallization of the matrix could have occurred by this fluid penetration and hydrothermal metamorphism. During or after the formation of deep-seated shear zones, a network of fractures formed in the overlying phyllites. Fluids derived from dioritic intrusions or externally derived hot hydrous fluids ascend through the shear zones, interact with the wall rocks, and finally escape along the fractures into the upper units. Eventually, these fluids are percolated parallel to the foliation plane, wherein the studied hornblendes crystallize. Selverstone and Munoz (1987) also demonstrated that in the Tauern Window from Eastern Alps fluid mobility or fluid movement occurred parallel to the foliation of the shear zone. The shape and distribution of hornblendes suggest that the fractures acted as pathways for the fluids. One of the most striking features of the studied rocks is gathering of hornblende crystals around the fractures (Figure 12), which is likely the result of a large volume of fluids circulating through these structures. The rapid growth of hornblende porphyroblasts removed H_2O from the fluids and resulted in a gradual increase in the CO_2 contents of the fluids. Sporadic calcites in the matrix may have been formed by these CO_2-rich fluids.

The Sanandaj–Sirjan zone has experienced several deformation phases, metamorphic events, and magmatism (Mohajjel et al., 2003; Hassanzadeh et al., 2008; Sheikholeslami, 2015). Numerous acidic intrusions have occurred from the Neoproterozoic (Hassanzadeh et al., 2008) to Eocene (Braud, 1987; Mahmoudi et al., 2011) in this zone. In the studied area, these intrusions could have acted as heat sources for the formation of the hornblende aggregates. In addition, several authors worked on granitic intrusions outcropped mainly in the northwestern and central parts of the Sanandaj–Sirjan zone (Mahmoudi et al., 2011; Alirezaei and Hssanzadeh, 2012; Azizi et al., 2015; Bayati et al., 2017). As reported by Sabzehei et al. (1997b), in the study area, Mesozoic units (Abkhamosh and Kahdan sedimentary formations) are not metamorphosed and they overlie the metamorphic complexes (such as the Gol-e-Gohar). It means that the Jurassic to Cretaceous magmatic–metamorphic events have not been severely affected the hornblende aggregates in the studied area.

6. Conclusions

1- The Gol-e-Gohar complex contains a succession of metabasites and metasedimentary (phyllites and slates) rocks intruded by granitoid igneous bodies.

2- Detailed field, petrography, and mineral chemistry investigations suggest that feather-textured hornblende aggregates and their host Garbenschiefer phyllites in this complex have been formed by relatively high-temperature hydrothermal metamorphism.

3- Hydrothermal metamorphism affected the highly strained mylonites and crystallized the hornblende radial aggregates under static conditions.

4- Fracture networks act as pathways through which the fluids ascend and penetrate into the phyllites and directly crystallize the hornblendes parallel to the foliation planes.

5- Granitoid intrusions could have been a source of heat for the fluids. The fluids leached Mg, Fe, and other essential elements from underlying metabasites.

Acknowledgments

The authors acknowledge financial support from Shahid Bahonar University of Kerman. We are grateful to Dr Shahram Shafiei for critical discussions.

References

Agard P, Omrani J, Jolivet L, Mouthereau F (2005). Convergence history across Zagros (Iran): Constraints form collisional and earlier deformation. Int J Earth Sci 94: 401-419.

Agard P, Omrani J, Jolivet L, Whitechurch H, Vrielynck B, Spakmam W, Monie P, Meyer B, Wortel R (2011). Zagros Orogeny: a subduction-dominated. Geol Mag 148: 692-725.

Alirezaei S, Hassanzadeh J (2012). Geochemistry and zircon geochronology of the Permian A-type Hasanrobat granite, Sanandaj–Sirjan belt: A new record of the Gondwana break-up in Iran. Lithos 151: 122-134.

Alt JC (1999). Very low-grade hydrothermal metamorphism of basic igneous rocks. In: Frey M, Robinson D, editors. Low-grade Metamorphism. Oxford, UK: Blackwell Science, pp. 169-201.

Arfania R, Shahriari S (2009). Role of southern Sanandaj-Sirjan zone in the tectonic evolution of the Zagros orogenic belt, Iran. Isl Arc 18: 555-576.

Azizi H, Najari M, Asahara Y, Catlos EJ, Shimizu M, Yamamoto K (2015). U–Pb zircon ages and geochemistry of Kangareh and Taghiabad mafic bodies in northern Sanandaj–Sirjan Zone, Iran: evidence for intra-oceanic arc and back-arc tectonic regime in Late Jurassic. Tectonophysics 660: 47-64.

Bayati M, Esmaeily D, Maghdour-Mashhour R, Lic XH Stern RJ (2017). Geochemistry and petrogenesis of Kolah-Ghazi granitoids of Iran: insights into the Jurassic Sanandaj-Sirjan magmatic arc. Chem der Erde 77: 281-302.

Berberian M, King GCP (1981). Towards a paleogeography and tectonic evolution of Iran. Can J Earth Sci 18: 210-265.

Berger A, Stunitz H (1996). Deformation mechanisms and reaction of hornblende: examples from the Bergell tonalite (Central Alps). Tectonophysics 257: 149-174.

Bevins RE, Robinson D (1994). A review of low grade metabasite parageneses. In: Hanquan W, Bai T, Yiqun L, editors. Very Low Grade Metamorphism: Mechanisms and Geological Applications. Beijing, China: The Seismological Press, pp. 1-8.

Biermann C (1977). The formation of sheaf-like aggregates of hornblende in garbenschiefer from the central Scandinavian Caledonides. Tectonophysics 39: 487-499.

Braud J (1987). La suture du Zagros au niveau de Kermanshah (Kurdistan iranien): Reconstitution palégéographique, evolution géodynamique, magmatique et structural. PhD, Université de Paris-Sud, Paris, France.

Bucher K, Grapes R (2011). Petrogenesis of Metamorphic Rocks. Berlin, Germany: Springer-Verlag.

Cathelineau M, Nieva D (1985). A chlorite solution geothermometer. The Los Azufres (Mexico) geothermal system. Contrib Mineral Petr 91: 235-244.

Coombs DS (1961). Some recent work on the lower grades of metamorphism. Aust J Earth Sci 24: 203-215.

Essaifi A, Capdevila R, Fourcade S, Lagarde JL, Ballèver M, Marigna CH (2004). Hydrothermal alteration, fluid flow and volume change in shear zones: the layered mafic–ultramafic Kettara intrusion (Jebilet Massif, Variscan belt, Morocco). J Metamorph Geol 22: 25-43.

Faryad SW, Hoinkes G (1999). Two contrasting mineral assemblages in the Meliata blueschists, Western Carpathians, Slovakia. Mineral Mag 63: 489-501.

Furnes H, Rosing M, Dilek Y, Wit M (2009). Isua supracrustal belt (Greenland)-A vestige of a 3.8 Ga suprasubduction zone ophiolite and the implications for Archean geology. Lithos 113: 115-132.

Graessner T, Schenk V (1999). Low-pressure metamorphism of Paleozoic pelites in the Aspromonte, Southern Calabria: constraints for the thermal evolution in the Calabrian crustal cross-section during the Hercynian orogeny. J Metamorph Geol 17: 157-172.

Hacker BR, Abers GA, Peacock SM (2003). Subduction factory, 1, Theoretical mineralogy, density, seismic wave speeds, and H_2O content. J Geophys Res 108: 1-26.

Hammarstrom JM, Zen EA (1986). Aluminum in hornblende: an empirical igneous geobarometer. Am Mineral 71: 1297-1313.

Hemley JJ, Montoya JW, Nigrini A, Vincent HA (1971). Some alteration products in the system CaO-Al_2O_3-SiO_2-H_2O. Society of Mining Geology. Japan, Special Issue 2: 58-63.

Hey MH (1954). A new review of the chlorites. Mineral Mag 30: 277-292.

Holland T, Blundy J (1994). Nonideal interactions in calcic amphiboles and their bearing on amphibole-plagioclase thermometry. Contrib Mineral Petr 116: 433-447.

Kelley DS, Malpas J (1996). Melt-fluid evolution in gabbroic rocks from the Hess Deep, Ocean Drilling Leg 147. In: Allan J, Gillis K, Mevel C, editors. Proceeding of the Ocean Drilling Program, Scientific Results. College Station, TX, USA: Ocean Drilling Program, pp. 213-226.

Kirby SH, Kronenberg AK (1987). Rheology of the lithosphere–selected topics. Rev Geophys 25: 1219-1244.

Kretz R (1983). Symbols for rock forming minerals. Am Mineral 68: 277-279.

Kruse R, Stunitz H (1999). Deformation mechanisms and phase distribution in mafic high-temperature mylonites from the Jotun Nappe, southern Norway. Tectonophysics 303: 223-249.

Leake BE, Woolley AR, Arps CES, Birch WD, Gilbert MC, Grice JD, Hawthorne FC, Kato A, Kisch HJ, Krivovichev VG et al (1997). Nomenclature of amphiboles: Report of the subcommittee on amphiboles of the International Mineralogical Association, Commission on New Minerals and Mineral Names. Can Mineral 35: 219-246.

Mahmoudi S, Corfu F, Masoudi F, Mehrabi B, Mohajjel M, (2011). U–Pb dating and emplacement history of granitoid plutons in the northern Sanandaj–Sirjan Zone, Iran. J Asian Earth Sci 41: 238-249.

Mohajjel M, Baharifar A, Moinevaziri H, Nozaem R (2006). Deformation history, micro-structure and P-T-t path in ALS bearing schist, southeast Hamadan, Sanandaj-Sirjan Zone, Iran. J Geol Soc Iran 1: 11-19.

Mohajjel M, Fergusson CL (2014). Jurassic to Cenozoic tectonics of the Zagros orogeny in the northwestern Iran. Int Geol Rev 53: 263-287.

Mohajjel M, Fergusson CL (2000). Dextral transpression in late Cretaceous continental collision, Sanandaj-Sirjan zone, Western Iran. J Struct Geol 22: 1125-1139.

Mohajjel M, Fergusson CL, Sahandi MR (2003). Cretaceous-Tertiary convergence and continental collision, Sanandaj-Sirjan zone, western Iran. J Asian Earth Sci 21: 397-412.

Omrani J, Agard P, Whitechurch H, Benoit M, Prouteau G, Jolivet L (2008). Arc magmatism and subduction history beneath the Zagros mountains, Iran: a new report of adakites geodynamic consequences. Lithos 106: 380-398.

Polat A, Hofmann AW, Rosing MT (2002). Boninite-like volcanic rocks in the 3.7–3.8 Ga Isua greenstone belt, West Greenland: geochemical evidence for intra-oceanic subduction zone processes in the early Earth. Chem Geol 184: 231-254.

Ranalli G, Murphy DC (1987). Rheological stratification of the lithosphere. Tectonophysics 132: 281-295.

Robinson P, Spear FS, Schumacher JC, Laird J, Klein C, Evans BW, Doolan BL (1982). Phase relations of metamorphic amphiboles: natural occurrence and theory. In: Veblen DR, Ribbe PH editors. Amphiboles: Petrology and Experimental Phase Relations. Mineralogical Society of America Rev Mineral Geochem 9B: 1-228.

Rose NM, Bird DK (1994). Hydrothermally altered dolerite dykes in East Greenland: implications for Ca-metasomatism of basaltic protoliths. Contrib Mineral Petr 116: 420-432.

Sabzehei M, Navazi M, Azizan H, Roshan Ravan J, Nazemzadeh M (1997b). Geological map of Khabr, Scale 1/100000. Geol Surv Iran, Tehran, Iran.

Sabzehei M, Navazi M, Eshraghi SA, Roshan Ravan J, Hamdi B, Seraj M (1997a). Geological map of Gol-e-Gohar, Scale 1/100000. Geol Surv Iran, Tehran, Iran.

Schumacher JC (2007). Metamorphic amphiboles: composition and coexistence. Rev Mineral Geochem 67: 359-416.

Sheikholeslami MR, Pique A, Mobayen P, Sabzehei M, Bellon H, Emami MH (2008). Tectono-metamorphic evolution of the Neyriz metamorphic complex, Quri-Kor-e-sefid area (Sanandaj-Sirjan zone, SW Iran). J Asian Earth Sci 31: 504-521.

Sheikholeslami MR (2015). Deformations of Palaeozoic and Mesozoic rocks in southern Sirjan, Sanandaj–Sirjan Zone, Iran. J Asian Earth Sci 106: 130-149.

Silantyev SA, Kostitsyn YA, Cherkashin DV, Dick HJB, Kelemen PB, Kononkova NN, Kornienko EM (2008). Magmatic and metamorphic evolution of the oceanic crust in the western flank of the MAR crest zone at 15°44′N: investigation of cores from sites 1275B and 1275D, JOIDES resolution Leg 209. J Petrol 16: 353-375.

Springer RK, Day HW (2002). Hydrothermal amphibole in subgreenschist facies mafic rocks, western Sierra Nevada, California. Schweiz Miner Petrog 82: 341-354.

Steffen K, Silverstone JS, Brearley A (2014). Episodic weakening and strengthening during synmetamorphic deformation in a deep-crustal shear zone in the Alps. Geol Soc London. Spec Publ 186: 141-156.

Stocklin J (1968). Structural history and tectonics of Iran: a review. Am Assoc Petr Geol B 52: 1229-1258.

Stokes MR, Wintsch RP, Southworth CS (2012). Deformation of amphibolites via dissolution-precipitation creep in the middle and lower crust. J Met Geol 30: 723-737.

Streit JE, Cox SF (1998). Fluid infiltration and volume change during mid-crustal mylonitization of Proterozoic granite, King Island, Tasmania. J Met Geol 16: 197-212.

Topus G (2006). Contact metamorphism around the Eocene Saraycık granodiorite, Eastern Pontides, Turkey. Turkish J Earth Sci 15: 75-94.

Tullis J, Yund R, Farver J (1996). Deformation-enhanced fluid distribution in feldspar aggregates and implications for ductile shear zones. J Geol 24: 63-66.